

GEOMETRY EFFECTS ON THE NONLINEAR OSCILLATIONS OF VISCOELASTIC CYLINDRICAL SHELLS

Zenon J. G. N. del Prado¹, Marco Amabili², Paulo B. Gonçalves³ and Frederico Da Silva¹

¹ Escola de Engenharia Civil, Universidade Federal de Goiás, UFG
Av. Universitária, s/n, Setor Universitário, 74605-200, Goiânia, GO, Brazil
e-mail: {zenon, silvafma}@ufg.br

² Department of Mechanical Engineering, McGill University
817 Sherbrooke Street West, H3A 0C3, Montreal, Canada
e-mail: marco.amabili@mcgill.ca

³ Catholic University of Rio de Janeiro, Department of Civil Engineering
Rua Marquês de São Vicente, 225, Gávea, 22453-900, Rio de Janeiro, RJ, Brazil
e-mail: paulo@puc-rio.br

Keywords: Cylindrical shells, viscoelastic material, Kelvin-Voigt model, lateral loads, non-linear vibrations.

Abstract. *In this work the influence of geometry, load and material properties on the non-linear vibrations of a simply supported viscoelastic circular cylindrical shell subjected to lateral harmonic load is studied. Donnell's non-linear shallow shell theory is used to model the shell, assumed to be made of a Kelvin-Voigt material type, and a modal solution with six degrees of freedom is used to describe the lateral displacements. The Galerkin method is applied to derive a set of coupled non-linear ordinary differential equations of motion. Obtained results show that the viscoelastic dissipation parameter has significant influence on the instability loads and resonance curves.*

1 INTRODUCTION

Circular cylindrical shells have been extensively used in modern industrial applications and have made their analysis an important research area in applied mechanics and biomechanics. Viscoelastic materials are frequently used in sandwich structures such as beams, plates and shells where damping is desired for a wide range of frequencies. However, in spite of a large number of studies on cylindrical shell dynamics, just a small number of these works is related to the analysis of viscoelastic shells.

An approximate theory for the linear dynamic response of viscoelastic cylindrical shells and cylindrical laminated composites with viscoelastic layers was proposed [1]. Also, the finite element method was applied to study the vibration of damped viscoelastic shells based on a first-order shear deformation theory including rotation around the normal [2]. A finite element formulation was developed to study the damping effects due to a constrained viscoelastic layer on the natural frequencies and loss factors of empty and fluid filled cylindrical shells [3].

Later, the dynamic behavior of viscoelastic cylindrical shells subjected to axial loads using the Von Kármán-Donnell non-linear shell theory, together with the Boltzmann laws to model the linear viscoelastic material was studied and observing the complex non-linear responses of the shell such as hyperchaos, chaos, strange attractors, and limit cycles [4]. The post buckling behavior of imperfect cylindrical panels considering a non-linear Schapery viscoelastic material was considered. It was possible to observe that, if linear viscoelastic and non-linear viscoelastic models are compared, the non-linear viscoelastic constitutive model predicts higher deflections than the linear viscoelastic ones [5].

After, a general methodology looking to describe the non-linear vibrations of viscoelastic shell structures, considering periodic or damped responses through the coupling of the harmonic balance method with one mode Galerkin discretization was considered [6]. The radial motions of compressible non-linearly viscoelastic cylindrical and spherical shells under lateral time-dependent pressures [7]. Considering temperature effects, the thermal post-buckled characteristics of cylindrical composite shells with viscoelastic layers by applying the finite element method considering transversal shear deformation and variable in-plane displacements through the thickness of the shell [8].

The problem of dynamic stability of viscoelastic, extremely shallow, circular cylindrical shells considering any viscoelastic functions as well as the inclusion of time-dependence of Poisson's ratio was also considered [9]. Forced vibrations of elastic and viscoelastic arches, panels and cylindrical shells using an asymptotic numerical method was studied in [10]. In the analysis, a mathematical formulation was developed in order to take into account various viscoelastic models in the frequency domain.

In a series of papers [11, 12, 13, 14, 15, 16] the vibrations and dynamic stability of viscoelastic cylindrical shells and cylindrical panels, with and without concentrated masses, using the Kirchhoff-Love hypothesis and Timoshenko theories and taking into account shear deformation and rotary inertia were considered.

Based on the profile of displacement fields of the core layer in static deformation, a new higher-order expansion of transverse and in-plane displacement fields in the thickness direction of the core layer was developed [17].

Recently, a detailed literature review of current studies on non-linear vibrations of shells where, a reduced number of studies dedicated to the analysis of viscoelastic cylindrical shells can be confirmed [18].

In the present paper, the influence of geometric relations, load and material properties on the non-linear vibrations and dynamic instability of a simply supported viscoelastic circular

cylindrical shells subjected to lateral harmonic load is studied. Donnell's non-linear shallow shell theory is used to model the shell, which is assumed to be made of a Kelvin-Voigt material type, and a modal solution with six degrees of freedom. The Galerkin method is applied to derive a set of coupled non-linear ordinary differential equations of motion that are, in turn, solved by the Runge-Kutta method. Results show that the viscoelastic dissipation parameter has a very significant influence on the instability loads and resonance curves.

2 MATHEMATICAL FORMULATION

Consider a perfect thin-walled simply supported circular cylindrical shell of radius R , length L and thickness h . The axial, circumferential and radial coordinates are denoted by x , $y = R\theta$ and z , respectively, and the corresponding displacements of the shell middle surface are denoted by u , v and w , as shown in Figure 1. The shell is assumed to be made of a Kelvin-Voigt viscoelastic material with initial Young's modulus E , Poisson ratio ν , and density ρ .

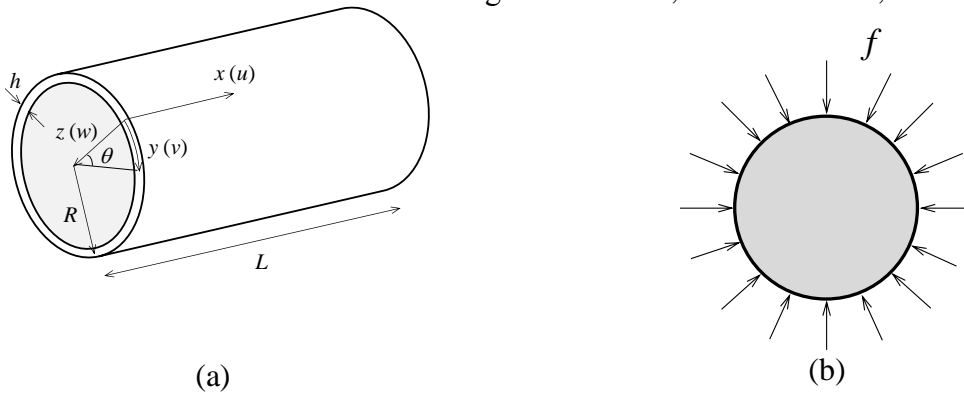


Figure 1: Shell characteristics. (a) Shell geometry; (b) Harmonic lateral pressure f .

The shell is subjected to the following harmonic lateral pressure:

$$f = F_L h^2 \rho \omega_o^2 \sin\left(\frac{m\pi x}{L}\right) \cos(n\theta) \cos(\omega_L t) \quad (1)$$

where F_L is the nondimensional coefficient of the amplitude of the load, ω_o is the natural frequency of the shell, m , the number of axial half-waves, n , the circumferential wave number, ω_L , the frequency of the load and t the time.

Based on Donnell shallow-shell theory, the middle surface kinematic relations are given, in terms of the three displacement components, by:

$$\begin{aligned} \varepsilon_{x,0} &= u_{,x} + \frac{1}{2} w_{,x}^2, & \varepsilon_{\theta,0} &= \frac{v_{,\theta}}{R} - \frac{w}{R} + \frac{1}{2} \frac{w_{,\theta}^2}{R^2}, & \gamma_{x\theta,0} &= \frac{u_{,\theta}}{R} + v_{,x} + w_{,x} \frac{w_{,\theta}}{R}, \\ \chi_{xx} &= -w_{,xx}, & \chi_{\theta\theta} &= -\frac{w_{,\theta\theta}}{R^2}, & \chi_{x\theta} &= -\frac{w_{,x\theta}}{R}, \end{aligned} \quad (2)$$

where $\varepsilon_{x,0}$ and $\varepsilon_{\theta,0}$ are the strains in the axial and circumferential directions, $\gamma_{x\theta,0}$ is the shearing strain component at a point on the shell middle surface, χ_{xx} and $\chi_{\theta\theta}$ are the curvature changes and $\chi_{x\theta}$ is the twist.

The strain components ε_{xx} , $\varepsilon_{\theta\theta}$ and $\gamma_{x\theta}$ at an arbitrary point of the shell are related to the middle surface strains $\varepsilon_{x,0}$, $\varepsilon_{\theta,0}$ and $\gamma_{x\theta,0}$ and to the changes in the curvature by the following relations:

$$\varepsilon_{xx} = \varepsilon_{x,0} + z\chi_{xx}, \quad \varepsilon_{\theta\theta} = \varepsilon_{\theta,0} + z\chi_{\theta\theta}, \quad \gamma_{x\theta} = \gamma_{x\theta,0} + z\chi_{x\theta}. \quad (3)$$

In this analysis, the viscoelastic behavior of the material is modeled in the base of the Kelvin-Voigt viscoelastic theory. This viscoelastic model can be represented by a viscous damper element and an elastic spring element connected in parallel as illustrated in Fig. 2.

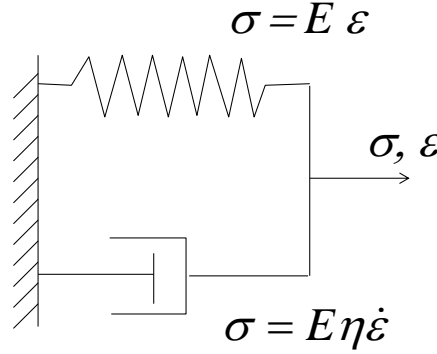


Figure 2. Kelvin – Voigt viscoelastic model

Considering the plane stress problem and the Kelvin-Voigt constitutive model of a viscoelastic material, the stress-strain relations can be written as [19]:

$$\sigma_{xx} = \frac{E}{1-\nu^2} \left[\varepsilon_{xx} + \nu \varepsilon_{\theta\theta} + \eta \frac{d}{dt} (\varepsilon_{xx} + \nu \varepsilon_{\theta\theta}) \right] \quad (4)$$

$$\sigma_{\theta\theta} = \frac{E}{1-\nu^2} \left[\varepsilon_{\theta\theta} + \nu \varepsilon_{xx} + \eta \frac{d}{dt} (\varepsilon_{\theta\theta} + \nu \varepsilon_{xx}) \right] \quad (5)$$

$$\sigma_{x\theta} = \frac{E}{2(1+\nu)} \left[\gamma_{x\theta} + \eta \frac{d}{dt} (\gamma_{x\theta}) \right] \quad (6)$$

where E is the Young's modulus, ν is the Poisson coefficient, t is the time and η is the coefficient of the viscoelastic dissipation parameter, also named retardation time, and it is measured in seconds.

Using the stress function F , the forces in the axial, circumferential and tangential directions are

$$N_x = \frac{1}{R^2} \frac{\partial^2 F}{\partial \theta^2}, \quad N_\theta = \frac{\partial^2 F}{\partial x^2}, \quad N_{x\theta} = -\frac{1}{R} \frac{\partial^2 F}{\partial x \partial \theta} \quad (7)$$

The non-linear equation of motion, based on the Donnell shallow shell theory, in terms of a stress function F , the lateral displacement w is given by:

$$\begin{aligned} & \frac{Eh^3}{12(1-\nu^2)} \left[\frac{\partial^4 w}{\partial x^4} + \frac{2}{R^2} \frac{\partial^4 w}{\partial x^2 \partial \theta^2} + \frac{1}{R^4} \frac{\partial^4 w}{\partial \theta^4} \right] + \frac{Eh^3}{12(1-\nu^2)} \eta \frac{\partial}{\partial t} \left[\frac{\partial^4 w}{\partial x^4} + \frac{2}{R^2} \frac{\partial^4 w}{\partial x^2 \partial \theta^2} + \frac{1}{R^4} \frac{\partial^4 w}{\partial \theta^4} \right] \\ & + c h \frac{\partial w}{\partial t} + \rho h \frac{\partial^2 w}{\partial t^2} = f + \frac{1}{R^2} \frac{\partial^2 F}{\partial \theta^2} \frac{\partial^2 w}{\partial x^2} - 2 \frac{1}{R^2} \frac{\partial^2 F}{\partial x \partial \theta} \frac{\partial^2 w}{\partial x \partial \theta} + \frac{\partial^2 F}{\partial x^2} \left(\frac{\partial^2 w}{R^2 \partial \theta^2} + \frac{1}{R} \right) \end{aligned} \quad (8)$$

where $c = 2\zeta\rho\omega_0$ (kg/m³ s) is the viscous damping coefficient, ζ is the viscous damping ratio of the shell and f is the radial pressure applied to the surface of the shell due to external

force. In equation (8) a global viscous damping has been introduced in addition to the viscoelasticity of the shell material.

The compatibility equation is given by

$$\begin{aligned} \frac{\partial^4 F}{\partial x^4} + \frac{2}{R^2} \frac{\partial^4 F}{\partial x^2 \partial \theta^2} + \frac{1}{R^4} \frac{\partial^4 F}{\partial \theta^4} = E h \left[-\frac{1}{R} \frac{\partial^2 w}{\partial x^2} + \frac{1}{R^2} \left(\frac{\partial^2 w}{\partial x \partial \theta} \right)^2 - \frac{1}{R^2} \frac{\partial^2 w}{\partial x^2} \frac{\partial^2 w}{\partial \theta^2} + \right. \\ \left. \eta \left(-\frac{1}{R^2} \frac{\partial^3 w}{\partial x^2 \partial t} \frac{\partial^2 w}{\partial \theta^2} - \frac{1}{R^2} \frac{\partial^2 w}{\partial x^2} \frac{\partial^3 w}{\partial \theta^2 \partial t} - \frac{1}{R} \frac{\partial^3 w}{\partial x^2 \partial t} + \frac{2}{R^2} \frac{\partial^3 w}{\partial x \partial \theta \partial t} \frac{\partial^2 w}{\partial x \partial \theta} \right) \right]. \end{aligned} \quad (9)$$

The simply supported out-of-plane (Eq. 10) and the in-plane (Eq. 11) boundary conditions are respectively given by:

$$w = 0, \quad M_x = 0 \quad \text{at } x = 0, L \quad (10)$$

$$N_x = 0, \quad v = 0 \quad \text{at } x = 0, L \quad (11)$$

For a formulation based on a stress function, the in-plane boundary conditions are satisfied on the average by introducing the following conditions, as justified, for example, in [20, 21, 22, 23, 24]

$$\int_0^{2\pi} N_x R d\theta = 0 \quad \text{at } x = 0, L \quad (12)$$

$$\int_0^{2\pi} \int_0^L N_{x\theta} R d\theta = 0 \quad \text{at } x = 0, L \quad (13)$$

Equation (12) assures a zero axial force N_x on the average, while Eq. (13) is satisfied when u and w are continuous in θ on average, and $v = 0$ on average at both ends.

In this work, the following modal expansion for the lateral displacements $w(x, \theta, t)$ in terms of the circumferential and axial variables is adopted:

$$\begin{aligned} w(x, \theta, t) = \xi_1(t) h \sin\left(\frac{m\pi x}{L}\right) \cos(n\theta) + \xi_2(t) h \sin\left(\frac{m\pi x}{L}\right) \sin(n\theta) + \\ \xi_3(t) h \sin\left(\frac{m\pi x}{L}\right) + \xi_4(t) h \sin\left(\frac{3m\pi x}{L}\right) + \xi_5(t) h \sin\left(\frac{5m\pi x}{L}\right) + \\ \xi_6(t) h \sin\left(\frac{7m\pi x}{L}\right) \end{aligned} \quad (14)$$

where $\xi_1(t)$, $\xi_2(t)$, $\xi_3(t)$, $\xi_4(t)$, $\xi_5(t)$ and $\xi_6(t)$ are the time-dependent non-dimensional modal amplitudes, where the shell thickness h has been used as non-dimensionalization parameter. This leads to a six-degrees-of-freedom reduced order model. This modal expansion satisfies the out-of-plane boundary conditions (10) and includes the basic vibration mode, the companion mode and four axi-symmetric modes and has been thoroughly tested in [20, 21, 24].

The solution for the stress function may be written as $F = F_h + F_p$, where F_h is the homogeneous solution and F_p , the particular solution. The particular solution F_p is obtained analytically by substituting the assumed form of the lateral displacement, Eq. (14), on the right-hand side of the compatibility equation, Eq. (9), and by solving the resulting partial differential equation together with the relevant boundary and continuity conditions.

The homogeneous part of the stress function can be written as (Amabili et al, 1999):

$$F_h = \frac{1}{2} \tilde{N}_x R^2 \theta^2 + \frac{1}{2} x^2 \left\{ \tilde{N}_\theta - \frac{1}{2\pi R L} \int_0^L \int_0^{2\pi} \frac{\partial^2 F_p}{\partial x^2} R d\theta dx \right\} - \tilde{N}_{x\theta} x R \theta \quad (15)$$

where \tilde{N}_x , \tilde{N}_θ and $\tilde{N}_{x\theta}$ are the in-plane restrain stresses at the ends of the shell.

Upon substituting the modal expressions for F and $w(x, \theta, t)$ into the equation of motion, Eq. (8), and applying the Galerkin method, a set of six non-linear ordinary differential equations is obtained in terms of the time-dependent modal amplitudes, $\xi_i(t)$.

In analysis, the following non-dimensional parameters are used for time and shell frequency:

$$\tau = \omega_o t; \quad \Omega = \omega_L / \omega_o \quad (16)$$

3 NUMERICAL RESULTS

Consider a simply supported viscoelastic cylindrical shell with the following physical and geometrical properties: $R = 0.2$ m, $L = 0.4$ m, $\rho = 1340.0$ kg/m³, $\nu = 0.195$, $E = 45.5e9$ N/m² [25], $\zeta = 0.001$.

To study the influence of geometry on nonlinear dynamic behavior of the orthotropic shells, Table 1 displays the selected L/R ratio, R/h ratios, associated longitudinal and circumferential wavenumber and natural frequencies which will be used on the foregoing analysis.

L/R	R/h	(m,n)	ω_o (rad/sec)
2,0	100	(1,5)	3447.29
	300	(1,7)	2007.06
	600	(1,8)	1427.86

Table 1: Selected shell geometries

To try to understand the influence of both the viscoelastic dissipation parameter and the lateral load on the non-linear dynamic behavior of the shell, several resonance curves and time responses have been computed. The bifurcation diagrams were obtained using Poncaré mapping and considering the excitation frequency as control parameter. The nondimensional coefficient of the amplitude of the lateral load F_L was assumed as 0.2; for the coefficient of the viscoelastic dissipation parameter of the Kelvin-Voigt model η , the following values were assumed: 0.0, 1.0e-5, 2.0e-5 and 3.0e-5 and 1.0e-4 s.

Figure 3 displays the resonance curves of driven mode for $F_L = 0.2$; $L/R = 2.0$; $R/h=100$ and increasing values of the dissipation parameter. As it can be observed in Fig. 3(a), for a shell without viscoelasticity ($\eta = 0.0$), as the frequency parameter Ω is increased the shell displays small amplitude period oscillations (1T). At excitation frequency near $\Omega = 0.90$ the shell displays a jump from small to large amplitude oscillations displaying softening behavior. As the value of Ω is increased, the shell shows a reduction of the amplitude of oscillations.

Now, when the viscoelastic dissipation parameter is considered ($\eta \neq 0$), the non-linear behavior of the shell is strongly influenced. Figure 3(b) shows the resonance curve for $\eta = 1.0e-5$ s and as the frequency parameter Ω is increased, the shell displays small amplitude 1T period oscillations. Again at a value close to $\Omega = 0.90$, the shell displays a jump to large amplitude oscillations with strong softening behavior. Then, for Ω between 0.72 and 0.77, the shell displays three different stable equilibrium points, which means that there will be three stable

attractors. At large amplitude a folding of the backbone curve (turning point) associated with large bending effects occurs.

When η is increased to 2.0×10^{-5} s as shown in Fig. 3(c), the resonance curve is again affected and it shows softening behavior but with smaller vibration amplitudes than for the previous case. Also, in Figs. 3(b) and 3(c) for $\Omega=1.0$ the shell displays a bifurcation point where the unstable path is linked to the large vibrations amplitudes path. Now, in Fig. 3(d) for $\eta = 3.0 \times 10^{-5}$ s, the shells displays only small amplitude vibrations without any jump.

Figure 4 displays the resonance curves for $F_L = 0.2$; $L/R = 2.0$; $R/h=300$ and increasing values of the dissipation parameter. Now, in Fig. 4(a) for $\eta = 0.0$, as the frequency parameter Ω is increased the shell displays small amplitude period oscillations (1T). At excitation frequency near $\Omega = 0.92$ the shell displays a jump from small to large amplitude oscillations displaying softening behavior, as can be observed, the vibrations amplitudes for this case are higher than those of Fig. 3(a) showing the great influence of geometric relations on the non-linear oscillations of the shell. For this case, it is also possible to observe a bifurcation point near to $\Omega = 1.00$ where stable solutions coexist.

Now, if dissipation parameter is considered ($\eta \neq 0.0$), Fig. 4(b) the shells depicts the resonance curve for $\eta = 1.0 \times 10^{-5}$ s, as can be observed, there is softening behavior with large amplitude 1T oscillations with similar behavior as Fig. 4(a). Now, if dissipation parameter is increased to $\eta = 2.0 \times 10^{-5}$ s as displayed on Fig. 4(c), the non-linear response of the shell is affected and the shell displays softening behavior with smaller amplitude oscillations and the coexistence of stable and chaotic vibrations. When dissipation parameter is increased up to $\eta = 3.0 \times 10^{-5}$ s as shown in Fig. 4(d), the system displays a jump with softening behavior but again with smaller vibration amplitudes than in previous cases.

Finally, Fig. 5 depicts the resonance curves considering $F_L = 0.2$; $L/R = 2.0$; $R/h=300$. In Fig. 5(a) the dissipation parameter is not considered ($\eta = 0.0$) and, as observed, the shell displays softening behavior with very large amplitude if compared with previous cases. In Fig. 5(b), Fig. 5(c) and Fig. 5(d) the shell always shows softening behavior but only with 1T stable oscillations. For $\eta = 3.0 \times 10^{-5}$ s as seen in Fig. 5(d), the amplitude of oscillations are smaller than in Fig. 5(b) or Fig. 5(c).

From these diagrams, it is possible to see the strong influence that geometry ratios and dissipation parameter have on the non-linear dynamic response of the shell. For a shell with low R/h ratio the shell displays smaller vibration amplitudes than a shell with high R/h ratio. When dissipation parameter is considered, for low values the amplitude of oscillations of the shell are increased even knowing that this parameter is a dissipation, for higher values of the parameter the vibration amplitudes of the shell will be reduced.

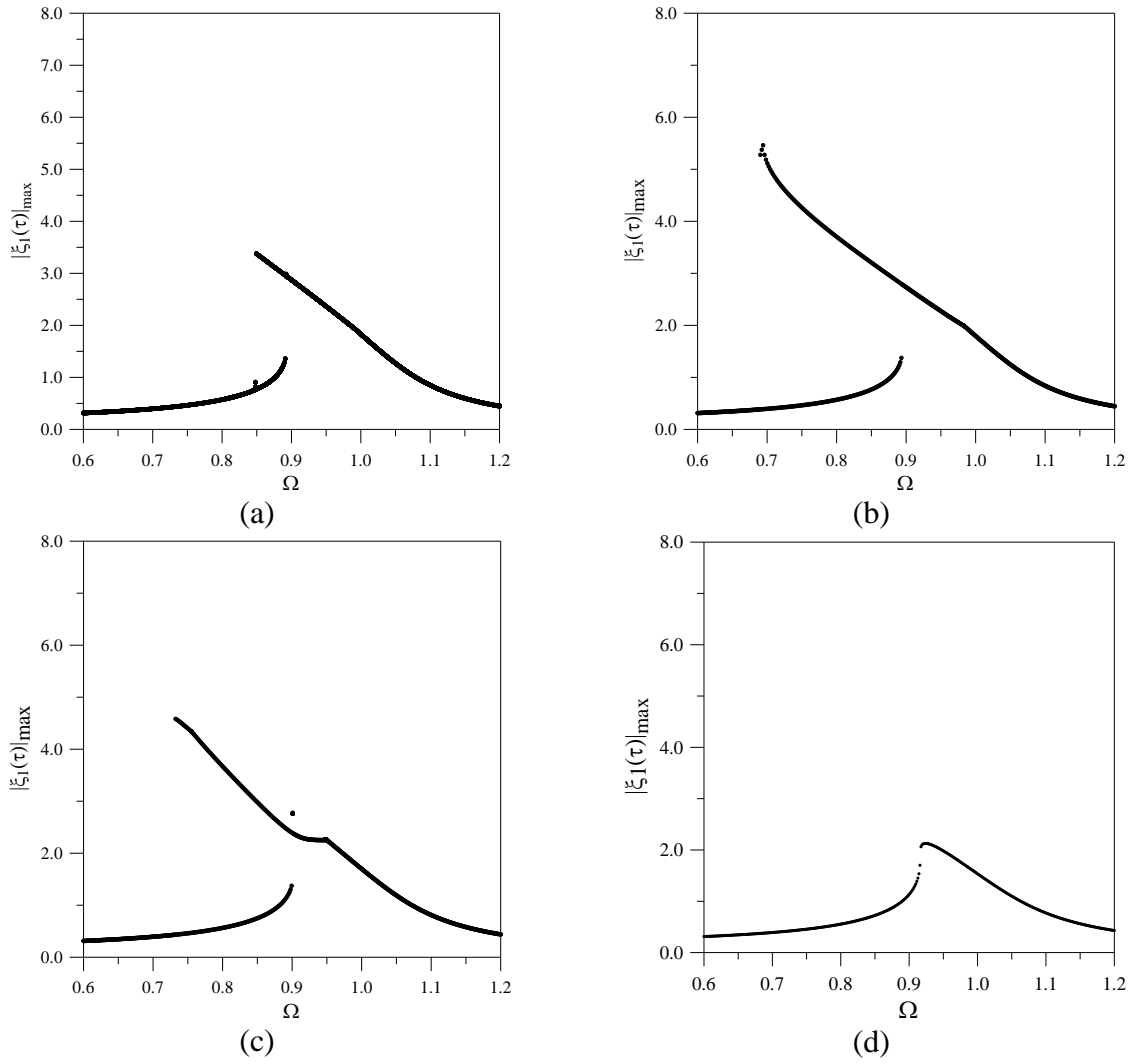
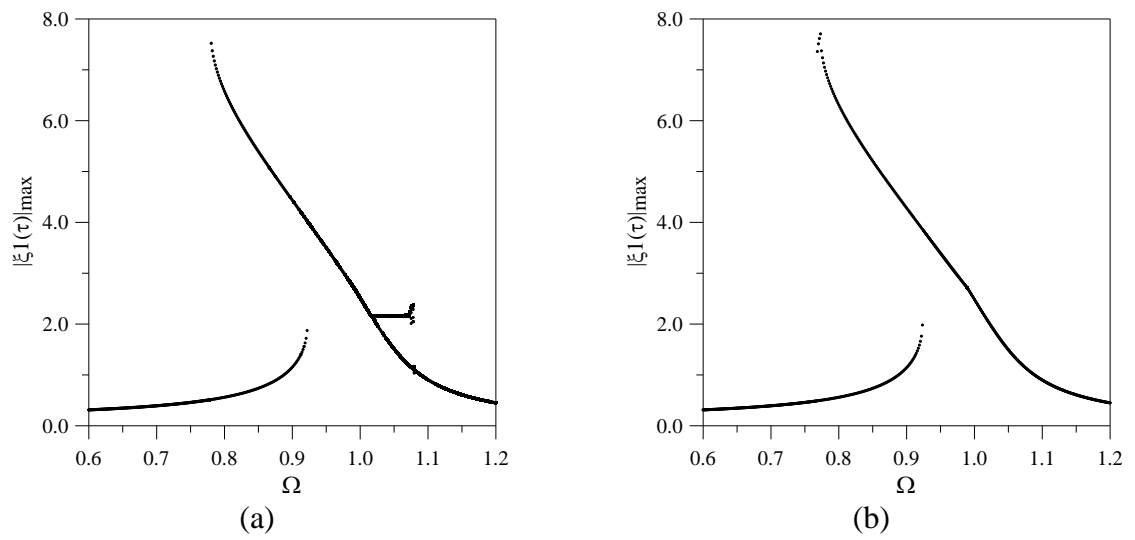


Figure 3. Resonance curves for $L/R = 2.0$ and $R/h = 100$. (a) $\eta = 0.0$; (b) $\eta = 1.0e-5s$; (c) $\eta = 2.0e-5s$; (d) $\eta = 3.0e-5s$.



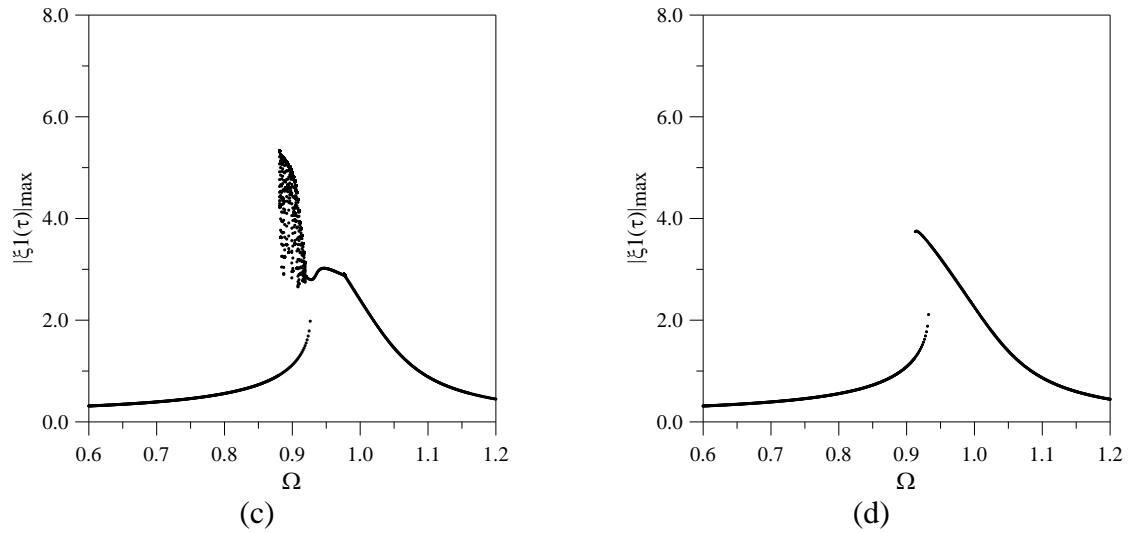


Figure 4. Resonance curves for $L/R = 2.0$ and $R/h = 300$. (a) $\eta = 0.0$; (b) $\eta = 1.0e-5s$; (c) $\eta = 2.0e-5s$; (d) $\eta = 3.0e-5s$.

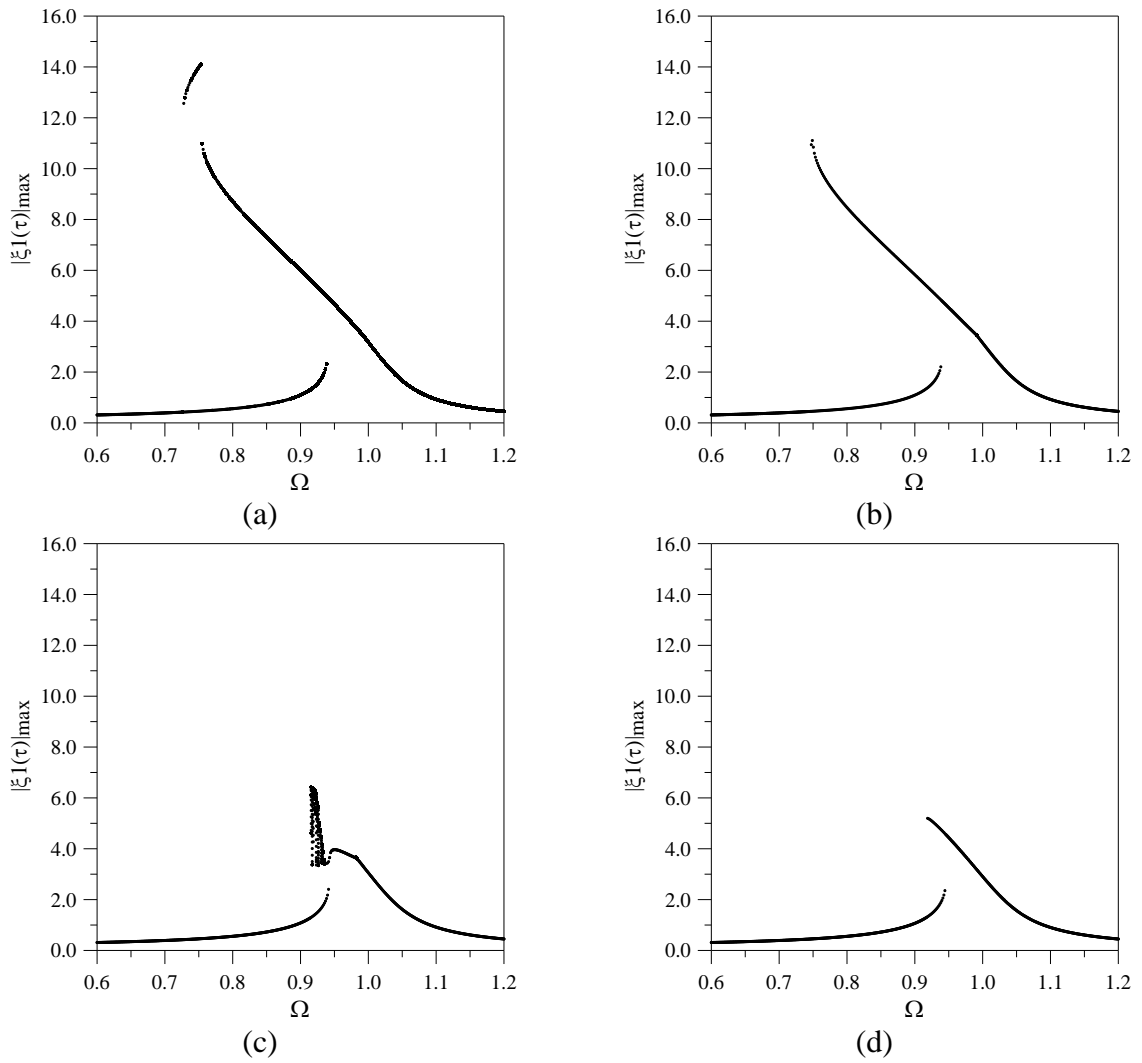


Figure 5. Resonance curves for $L/R = 2.0$ and $R/h = 600$. (a) $\eta = 0.0$; (b) $\eta = 1.0e-5s$; (c) $\eta = 2.0e-5s$; (d) $\eta = 3.0e-5s$.

4 CONCLUSIONS

In this work, the non-linear vibrations analysis of a viscoelastic Kelvin-Voigt simply supported cylindrical shell subjected to lateral time dependent loads is analyzed. To model the shell, the Donnell's non-linear shallow shell theory is applied and an expansion with 6 degrees of freedom is used to describe the lateral displacements. Results show that the inclusion of the viscoelastic dissipation parameter η of the Kelvin-Voigt material affects strongly the non-linear response of the shell.

It is observed that the complexity of the non-linear response and consequently the number of bifurcations, non-linear paths and coexisting solutions depends on the value of the viscoelastic dissipation parameter.

For higher values of the dissipation parameter, the shell only displays small amplitude vibrations without jumps, hysteresis and multiple solutions. This illustrates the beneficial effect of viscoelasticity in reducing large amplitude unwanted vibrations. The amplitudes of vibrations obtained in the numerical results calls to the necessity to use a more refined shell theory to describe the non-linear dynamic behavior with good accuracy.

ACKNOWLEDGMENTS

This work was made possible by the support of the Brazilian Ministry of Education – CNPq and FAPERJ-CNE and NSERC Discovery Grant, Discovery Accelerator Supplement and Canada Research Chair.

REFERENCES

- [1] Mengi Y, Birlik GA. A refined dynamic theory for viscoelastic cylindrical shells and cylindrical laminated composites, Part 1: General Theory. *Journal of Sound and Vibration*, **103**, 55-67, 1989.
- [2] Rikards R, Chate A. Vibration and damping analysis of laminated composite and sandwich shells. *Mechanics of Composite Materials and Structures*, **4**, 209-232, 1997.
- [3] Ramasamy R, Ganesan N. Vibration and damping analysis of fluid-filled orthotropic cylindrical shells with constrained viscoelastic damping. *Computers and Structures*, **70**, 363-376, 1999.
- [4] Cheng C, Zhang N. Dynamic behavior of viscoelastic cylindrical shells under axial pressure, *Applied Mathematics and Mechanics*, **22**, 1-9, 2001.
- [5] Cederbaum G, Touati D. Postbuckling analysis of imperfect non-linear viscoelastic cylindrical panels. *International Journal of Non-Linear Mechanics*, **37**, 757-762, 2002.
- [6] Boutyour E H, Daya EM, Michel P. A harmonic balance method for the non-linear vibration of viscoelastic shells. *C. R. Mecanique*, **334**, 68-73, 2006.
- [7] Antman SS, Lacarbonara W. Forced Radial Motions of Nonlinearly Viscoelastic Shells. *Journal of Elasticity*, **96**, 155-190, 2009.
- [8] Shina W, Leeb S, Ohc I, Lee I. Thermal post-buckled behaviors of cylindrical composite shells with viscoelastic damping treatments. *Journal of Sound and Vibration*, **323**, 93-111, 2009.

- [9] Ilyasov MH. Parametric vibrations and stability of viscoelastic shells. *Mechanics of Time-Dependent Materials*, **14**, 153–171, 2010.
- [10] Abdoun F, Azrar L, Daya EM. Damping and Forced Vibration Analyses of Viscoelastic Shells, *International Journal for Computational Methods in Engineering Science and Mechanics*, **11**, 109–122, 2010.
- [11] Eshmatov BK, Khodjaev DA. Non-linear vibration and dynamic stability of a viscoelastic cylindrical panel with concentrated mass. *Acta Mechanica*, **190**, 165–183, 2007a.
- [12] Eshmatov BK. Nonlinear vibrations of viscoelastic cylindrical shells taking into account shear deformation and rotatory inertia. *Nonlinear Dynamics*, **50**, 353–361, 2007b.
- [13] Eshmatov BK. Dynamic stability of viscoelastic circular cylindrical shells taking into account shear deformation and rotatory inertia. *Applied Mathematics and Mechanics*, **28**, 1319–1330, 2007c.
- [14] Eshmatov BK, Khodzhaev DA. Non-linear vibration and dynamic stability of a viscoelastic cylindrical panel with concentrated mass. *Acta Mechanica*, **190**, 165–183, 2007d.
- [15] Eshmatov BK, Khodzhaev DA. Dynamic stability of a viscoelastic cylindrical panel with concentrated masses. *Strength of Materials*, **40**, 491–502, 2008.
- [16] Eshmatov BK. Nonlinear vibrations and dynamic stability of a viscoelastic circular cylindrical shell with shear strain and inertia of rotation taken into account. *Mechanics of Solids*, **44**, 421–434, 2009.
- [17] Mohammadi F, Sedaghati R. Vibration analysis and design optimization of viscoelastic sandwich cylindrical shell. *Journal of Sound and Vibration*, **331**, 2729–2752, 2012.
- [18] Alijani F, Amabili M. Non-linear vibrations of shells: A literature review from 2003 to 2013. *International Journal of Non-Linear Mechanics*, **58**, 233–257, 2013.
- [19] Esmailzade E, Jalali MA. Nonlinear Oscillations of Viscoelastic Rectangular Plates. *Nonlinear Dynamics*, **18**, 311–319, 1999.
- [20] Amabili M. *Nonlinear Vibrations and Stability of Shells and Plates. 1st Editon*. Cambridge University Press, 2008.
- [21] Amabili M, Pellicano F, Païdoussis MP. Non-linear dynamics and stability of circular cylindrical shells containing flowing fluid. Part I: Stability. *Journal of Sound and Vibration*, **225**, 655–699, 1999.
- [22] Stavridis L, Armenàkas A. Analysis of Shallow Shells with Rectangular Projection: Theory. *ASCE Journal of Engineering Mechanics*, **114**, 923–942, 1988.
- [23] Breslavsky ID, Avramov KV. Effect of boundary condition nonlinearities on free large-amplitude vibrations of rectangular plates. *Nonlinear Dynamics*, **74**, 615–627, 2013.
- [24] Del Prado Z, Argenta AL, Da Silva F, Gonçalves PB. The effect of material and geometry on the non-linear vibrations of orthotropic circular cylindrical shells. *International Journal of Non-Linear Mechanics*, **66**, 75–86, 2014.
- [25] Balkan D, Mecitoglu Z. Nonlinear dynamic behavior of viscoelastic sandwich composite plates under non-uniform blast load: *Theory and experiment*. *International Journal of Impact Engineering*, **72**, 85–104, 2014.